ISSN 1392–1320 MATERIALS SCIENCE (MEDŽIAGOTYRA). Vol. 28, No. 3. 2022

DFT Based Material Computations of Metal-doped and Pure Carbon Nanodots for Examining their Enhancement of Sulfur Dioxide Adsorption

Mikail ASLAN *

Department of Metallurgical and Material Science Engineering, Gaziantep University, Gaziantep, 27310, Turkey

crossref http://10.5755/j02.ms.29540

Received 03 August 2021; accepted 12 October 2021

Carbon nanodots, one of the last members of the nanocarbon family, show superior properties, such as low-cost production, good conductivity, and optical properties, nontoxic behavior, high biocompatibility, and eco-friendly nature. Understanding the effect of metal doping on the modification of the electronic structure of carbon nanodots is critical for enlarging its potential applications. In the present study, in terms of structural, energetic, and electronic analyses, X-doped carbon nanodot structures (X = B, N, Si, Al, Co, Au, Pd, and Pt) and their SO_2 adsorption abilities were examined comprehensively by employing DFT. Results depict that embedding the heavy impurity metals (Pd, Pt) to the nanodot structures does not improve the SO_2 sensing ability of carbon nanodot materials relatively. However, the doping of the low concentrated metals to the carbon nanodots may be one of the best ways for enhancing the SO_2 trapping ability of the carbon nanodot materials since the calculated results having high adsorption energy values indicate SO_2 gas molecule is easily adsorbed on the surface of doped carbon nanodots. This means higher adsorption capability compared to pure ones. Thus, it is suggested that the doped carbon nanodots consisting of B, Si, and N impurity atoms may be good candidates for effective SO_2 sensing (adsorptions).

Keywords: nanomaterials, Lowden charges, doped carbon nanodots (carbon quantum dots), new type carbon-based materials, SO_2 sensing.

1. INTRODUCTION

Sulfur dioxide (SO_2) is considered one of the widespread gaseous pollutants [1] due to its toxic effect on Earth's atmosphere. Industrial complexes [2], power plants [3], volcanoes [4], households [5], and sulfur-bearing fossil fuels in automobile engines [6] are the main sources of this gas. SO_2 coupling with air in the atmosphere leads to the formation of acidic rains [7]. Some problems, such as corroding metals and buildings [8], acidizing rivers and lakes [9], and destroying soil [10] and vegetation [11] are the consequence of these acidic rains.

In terms of environmental safety and industrial control, their monitoring has been considerably increased for detecting sulfur dioxide. This has been recently led to the development of many SO_2 trapping systems. Chromatography [12], electrochemical analysis [13], and spectroscopy [14, 15] are some of the techniques used for SO_2 sensing. On the other hand, high-cost production, time-consuming, and the need for sophisticated measuring types of equipment are one of the disadvantages of these methods [16]. Alternatively, chemical sensors [17] have been developed. On the other hand, this technique has some drawbacks, such as lack of selectivity, high working temperatures, and high response times. To overcome this, nanomaterials were incorporated into these new sensor systems. In recent years, carbon-based materials including carbon nanoparticles [18], carbon nanofibers [19], carbon nanotubes(CNT) [20], fullerenes [21], graphenes [22], and especially carbon dots [23] have been using as sensing materials owing to their high sensing capability. Iijima [24] conducted a study of CNT-based chemical sensors by using Density Functional Theory (DFT) technique. CNT-based sensors have superior properties, such as faster response, higher sensitivity, smaller size, and lower working temperature when compared to traditional sensors. Nagarajan et al. [25] examined the adsorption ability of SO_2 upon hydrogenated graphene nanosheets and nanotubes. It was suggested in their studies that for monitoring different types of small gas molecules, such as NO_2 and SO_2, the chair typed graphene nanosheets and nanotubes, with edges saturated by hydrogen atoms can be preferred. Even with their advantages, some performance problems, such as selectivity to determine gaseous substances may be seen in these systems. Embedding or doping of impurity atom(s) is one of the techniques that get better sensing ability and selectivity. Yoosefian et al. [26] conducted a study of SO_2 adsorption on Pt-doped and Au-doped single-walled carbon nanotube (SWCNT). SO_2 adsorbed on Au/SWCNT and Pt/SWCNT indicate strong chemisorptions. Kim et al. [27] studied the adsorption of SO_2 on boron and nitrogen-doped graphene. SO_2 weakly interacted with N-doped graphenes with low adsorption energies and long distances between SO_2 and graphynes whereas SO_2 indicated strong adsorptions with B-doped graphenes.

In this paper, the ab initio based DFT technique used for the material investigation at the atomic/nanoscale level has been employed for elucidating the details of SO_2 adsorption, dopant effects, charge transformation, and crystal arrangements of pure and N-doped carbon nanodot particles (N = B, N, Si, Al, Co, N, Au, Pd, and Pt).

* Corresponding author. Tel.: +90(342)360 1200; fax: +90(342)360 1013.
E-mail address: *aslanm@gantep.edu.tr* (M. Aslan)

2. METHODS

CNDs are small parts of graphene sheets with quasi-zero-dimensional (0D). Ideal CNDs consist of only a single atomic layer. In the present study, CNDs that include 7 hexagonal rings and a total of 36 atoms were modeled with one single layer. The edges of the structure are saturated with 12 hydrogen atoms to eliminate the edge effects. To investigate the carbon-based materials at the atomic/nanoscale level, the DFT method was preferred by employing the Quantum Espresso (QE) packages that is a software program for atomic or nanoscale material modeling. The plane-wave projector-augmented wave method was implemented with the Broyden–Fletcher–Goldfarb–Shanno (BFGS) algorithm that is one of the ways for numerical optimizations. The PAW-PBE potential in the generalized gradient approximation (GGA) was used in the geometric optimizations. 1 × 1 × 1 k mesh point grids were preferred to optimize the structures. The adequate energy cutoff convergence criterion was chosen with a value of 200 R_y. The value of mixing beta is 0.5, which is used for improving convergence. The optimization is stopped and completed when differences between energies and total forces for successive structures become less than 10^{-4} R_y and 10^{-3} R_y/a_0, respectively. Energy and energy gradient convergences were preferred as 1×10^{-6} Hartree and 5×10^{-5} Hartree/a_0, respectively. The optimizations were done in a tetragonal supercell of 12 × 12 × 20 Å. A large vacuum space along z-direction in the unit cell was preferred to avoid spurious image interactions. Moreover, the effect of the van der Waals (vdW) was regarded in the structure calculations by employing the empirical correction scheme of Grimme's DFT-D3 technique [28]. With the interatomic potentials of the $C_6 \cdot R^{-6}$ form, dispersion effects consisting of a dispersive force modification are taken into account for GGA-PBE pseudopotentials. This provides easy energy decomposition to *vdW* and electronic parts during optimizations. Furthermore, the *vdW* corrections are described as simple pair-wise force fields, which are used in several popular DFT functional for structure optimizations.

3. RESULTS AND DISCUSSION

3.1. Doped carbon nanodots

The physical and chemical properties and performance of CND can be modified by introducing impurity (dopant) atoms since those strongly depend upon the bonding configurations of doped CND [29]. Embedding impurity atoms to structures with low concentrations, such as less than atomic 1 % has been of great interest for experimental purposes [30]. In the president study, dopant atoms were initially located at the center position of the CND structures and the doped structures were optimized to find the best energetic structures. Fig. 1 indicates the top-viewed geometric modeling of doped CND. The structures of all CNDs are not importantly distorted by the introduction of impurity atoms. This can be explained by the strong bonding strengths between CND atoms. Similar results were seen in the study [31]. The N, Si, and Pd dopings affect the first neighbors of the defect site and the second neighbors, leading to the changes of C–C distances. The third neighbors were distorted little. Thus, the distortions are mainly restricted to the second neighbors. Moreover, results depict that Al, Au, Co and Pd impurity atoms lead to weak interactions with the CND surfaces, see Fig. 1.

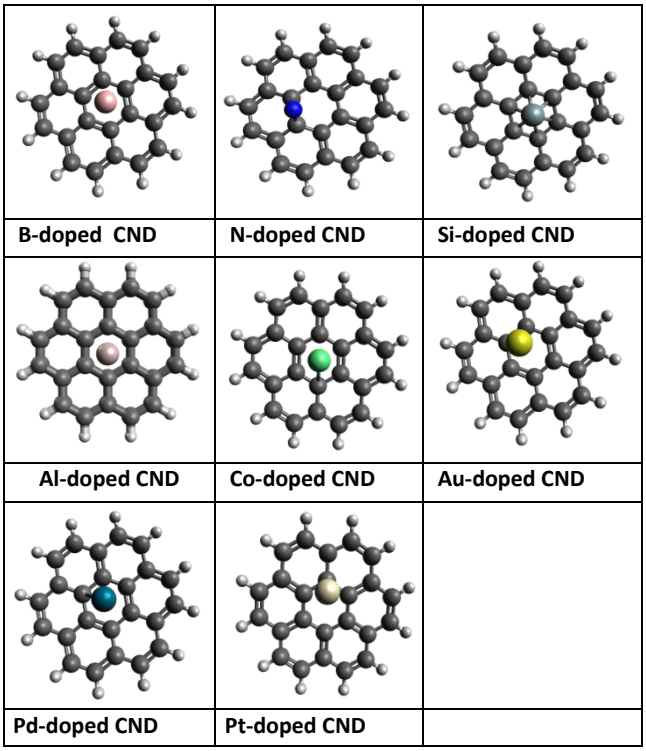

Fig. 1. The model of doped carbon nanodots(CND) with substitutional impurity atom

The optimized structures reveal that the studied impurity atoms except for N, Au, and Pt occupy the near central positions of the hexagonal ring of CND structures. In the study of Gecim et. al. [32], similarly with the Pt atom, Ga and Ge atoms occupied the central position of the graphene structures. Table 1 indicates the interaction tendencies of the impurity atoms upon CND surfaces. In addition, the dopant ability, E_{doped} is given as

$$E_{doped} = -E_{all} + E_{dopant} + E_{surface}, \quad (1)$$

where E_{all}, E_{dopant}, and E_{surface} mean the lowest energy values of all substrate, dopant atom, and CND surface, respectively. Nitrogen-doped carbon nanodot shows the strongest doping tendency, see Fig. 2. This may be related to the high relative electronegative value of this element that allows easiness for adequate attractive forces on carbon and hydrogen atoms. To analyze the charge transfers between CND and the impurity atoms, a Lowden charge analysis [29] of the transferred electrons was used. The charge gain or loss are calculated according to the difference between the Lowden charge of impurity atoms in the structures and free impurity atoms.

Table 1. The doping tendency and charge loss of the given dopant atoms upon the carbon nanodot surface. Positive charge means charge gainings

Dopants	B	N	Si	Al	Au	Co	Pd	Pt
E_{doped}, eV	0.34	3.03	0.38	0.44	2.12	0.02	0.79	1.29
Δq, e	– 0.04	0.28	– 0.19	0.47	0.25	0.11	– 0.11	0.01

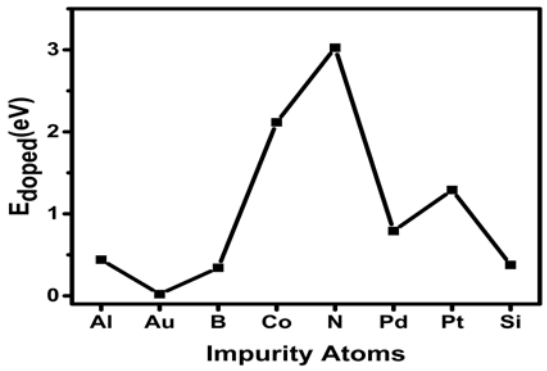

Fig. 2. The doping ability of each given atoms to carbon nanodot surface

Positive charge means charge gaining. The analysis indicates that although the Al atom among doped structures has the biggest relative charge gain, it could not provide adequate doping tendency due to its relatively heavy mass. On the other hand, B, Pd, and Si atoms lose their charges relatively slightly after the interactions with the surfaces.

3.2. SO_2 adsorption

The adsorption characteristics of SO_2 were investigated to understand the details of the adsorption ability upon the studied CNDs. The geometric structures of SO_2 adsorptions on the CNDs are shown in Fig. 3.

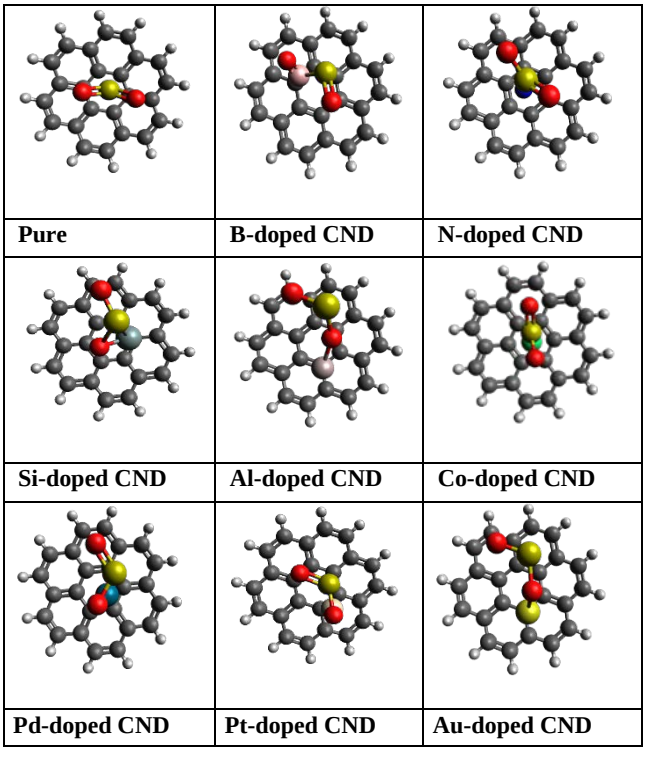

Fig. 3. The model of SO_2 adsorbed carbon nanodots (CND) with substitutional impurity atom

It is expected that metal-doped carbon structures lead to an increase in the value of SO_2 adsorption strength since in the previous studies [34], the metal addition but not all metals to the carbon structures may enhance the adsorption ability of S and N atoms. The SO_2 is adsorbed on the center of the surface of the pure CNDs. This is seen in the study conducted by Mirzaei et al. [35]. Their study indicated that the gas molecule was located almost at the middle of the surface, approving the appropriate size of the surface for such molecular adsorption process. In the present study, results indicate that different types of configurations, such as S-atom, O-atom and both of them were found in the SO_2 adsorptions of the metal-doped structures. As a comparison of SO_2 adsorption on pure CND surface, Al, Pt, and Au doped CNDs show similar SO_2 adsorption characteristics (O-down adsorptions). This can be explained by the weak interactions of SO_2 on the surfaces doped by Al and Au atoms. On the other hand, pure, N, Pt, and Co-doped CNDs indicate different adsorption characteristics (S-down adsorptions), Pd and Si show both S and O-down adsorptions and in the B-doped CNDs, SO_2 dissociation is observed.

Furthermore, the CND surfaces are not affected considerably due to the SO_2 adsorptions. This is because CNDs have strong carbon bondings. Thus, important defects and distortions on the surface were not observed. On the other hand, The geometric structures of SO_2 are distorted importantly in the B and N doped CNDs. In addition, the SO_2 traping ability, E_{trap} is given as

$$E_{trap} = -E_{all}+E_{SO_2}+E_{surface}, \quad (2)$$

where E_{all}, E_{SO_2} and $E_{surface}$ mean the lowest energy values of all substrate, SO_2 molecule and CND surface, respectively. Table 2 indicates the SO_2 interaction strength on the carbon nanodot surfaces. As compared to doped carbon nanodot particles, pure CND shows low adsorption ability.

Table 2. The SO_2 trapping values of the given structures

Material	Pure	B	N	Si	Al	Co	Au	Pd	Pt
E_{SO_2}, eV	0.01	6.44	4.53	5.39	3.21	2.14	0.80	1.61	2.46

This shows that impurity atoms with low concentrations can improve the SO_2 trapping ability of the carbon nanodot particles significantly. Furthermore, the SO_2 trapping trends of the structures are given in Fig. 4. The best trends for SO_2 adsorption are seen in the structures doped by B, Si, and N impurity atoms. The impurity atom is very important for enhancing SO_2 sensing. This was seen in the study of the interaction of SO_2 onto boron Ni-decorated $B_{12}P_{12}$ nanoclusters [36]. It may be concluded heavy doped metals such as Pd and Pt are not efficient as light metals to enhance the SO_2 trapping ability of the CND surfaces.

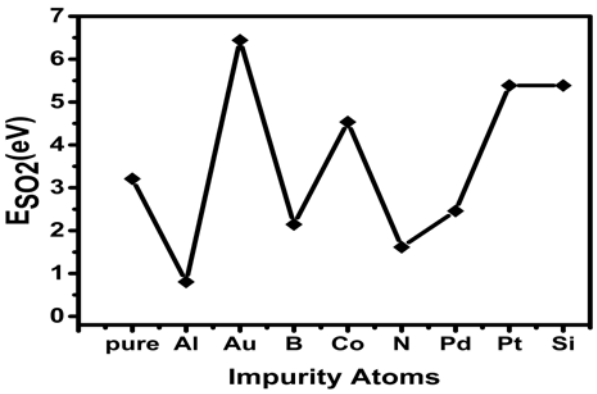

Fig. 4. The SO_2 sensing ability of the doped and pure carbon nanodots

4. CONCLUSIONS

A computational material study based on the first principle calculations was applied for the investigation of the doped carbon nanodots and their SO_2 trapping abilities at the nanoscale level. Quantum Espresso software package that is used for ab initio material modeling technique was preferred. In terms of microstructural evaluation, impurity atoms and SO_2 molecules do not provide adequate driving forces to alter the geometric structures of the CNDs considerably. This leads to limit the formation of more defects and distortions on the structures. Results indicate that all impurity atoms except for N and Pt are located in the near central positions of the hexagonal ring of the CND structures. The highest doping tendency was seen in the N-doped structures. This may be due to the high charge sharing/mass ratio, allowing for strong bonding formation between them. Furthermore, It was found that the SO_2 trapping strengths of these carbon-based nanomaterials are in the order B > Si > N > Al > Pt > Co > Pd > Au > pure. This indicates that the introduction of impurity atoms with low concentrations to the structures may be one of the efficient ways that improve the adsorption ability of the carbon nanodot structures. On the other hand, when compared to light metals, heavy metals are not good candidates that enhance the SO_2 trapping ability of the CNDs. Hence, this investigation suggests furthering experimental studies that B, Si, and N doped carbon nanodots can be used as an adsorbent that helps control and capture SO_2 harmful gases. In future work, for improving adsorption ability, the effect of the different arrangements of carbon structures, such as pristine, fullerene-like cages and nanotubes may be studied. For instance; see the studies [37-38]. Moreover, another nanoparticles [39-40] may be studied for this subject.

REFERENCES

1. **Landim, A.A., Teixeira, E.C., Agudelo-Castañeda, D., Schneider, I., Silva, L.F.O., Wiegand, F., Kumar, P.** Spatio-Temporal Variations of Sulfur Dioxide Concentrations in Industrial and Urban Area Via a New Statistical Approach *Air Quality, Atmosphere & Health* 11 2018: pp. 801 – 813. https://doi.org/10.1007/s11869-018-0584-2
2. **Lee, H.D., Yoo, J.W., Kang, M.K., Kang, J.S., Jung, J.H., Oh, K.J.** Evaluation of Concentrations and Source Contribution of PM10 and SO_2 Emitted From Industrial Complexes in Ulsan, Korea: Interfacing of the WRF–CALPUFF Modeling Tools *Atmospheric Pollution Research* 5 2014: pp. 664 – 676. https://doi.org/10.5094/APR.2014.076
3. **Karplus, V.J., Zhang, S., Almond, D.** Quantifying Coal Power Plant Responses to Tighter SO_2 Emissions Standards in China *Proceedings of the National Academy of Sciences* 115 2018: pp. 7004 – 7009. https://doi.org/10.1073/pnas.1800605115
4. **Lamotte, C., Marécal, V., Guth, J.** Update of the Volcanic Sulfur Emission Inventory in MOCAGE CTM and its Impact on the Budget of Sulfur Species in the Atmosphere *In EGU General Assembly Conference Abstracts*, 2020: pp. 4791.
5. **Seow, W.J., Downward, G.S., Wei, H., Rothman, N., Reiss, B., Xu, J., Bassig, B.A., Li, J., He, J., Hosgood, H.D., Wu, G., Chapman, R.S., Tian, L., Wei, F., Caporaso, N.E., Vermeulen, R., Lan, Q.** Indoor concentrations of nitrogen dioxide and sulfur dioxide from burning solid fuels for cooking and heating in Yunnan Province, China *Indoor Air* 26 2016: pp. 776 – 783. https://doi.org/10.1111/ina.12251
6. **Salahudin, S.N., Abdullah, M.M., Newaz, N.A.**. Emissions: sources, policies and development in Malaysia *International Journal of Education and Research* 1 2013: pp. 1 – 12.
7. **Lan, H.C., Zou, Y.T., Wang, Y.C., Cheng, N.N., Xu, W.L., Peng, H.L., Huang, K., Kong, L.Y., Du, J.** Meso-Macroporous Polymer Densely Functionalized with Tertiary Amine Groups as Effective Sorbents for SO_2 Capture *Chemical Engineering Journal* 2021: pp. 129699. https://doi.org/10.1016/j.cej.2021.129699
8. **Hutauruk, B.C., Martono, D.N., Sodri, A.** Risk and Impact Control of PM2. 5 and SO2 Exposure of Power Plant to Communities (A Case Study in the Steam Power Plant Babelan Bekasi) *Jurnal Kesehatan Lıngkungan* 13 2021: pp. 121 – 131. http://dx.doi.org/10.204,çiş73/jkl.v13i2.2021.121-131
9. **Liu, X.Y., Zhang, J.M., Xu, K.W., Ji, V.** Improving SO_2 Gas Sensing Properties of Graphene by Introducing Dopant and Defect: A First-Principles Study *Applied Surface Science* 313 2014: pp. 405 – 410. https://doi.org/10.1016/j.apsusc.2014.05.223
10. **Khurramovna, D.M., Madaminovich, K.J.** Contamination of Shale and Sandy Soils with Industrial Waste *International Journal of Modern Agriculture* 10 2021: pp. 414 – 417.
11. **Nassar, R.F.** Evaulation of a Model for Urban Vegetation Barriers' Effects on Air Pollution *Preprint* 2021: pp. 1 – 9. https://doi.org/10.20944/preprints202101.0170.v1
12. **Nonomura, M., Hobo, T.** Simultaneous determination of Sulphur Oxides, Nitrogen Oxides and Hydrogen Chloride in Flue Gas by Means of an Automated Ion Chromatographic System *Journal of Chromatography A* 804 1998: pp. 151 – 155. https://doi.org/10.1016/S0021-9673(98)00096-X
13. **Fergus, J.W.** A Review of Electrolyte and Electrode Materials for High Temperature Electrochemical CO_2 and SO_2 Gas Sensors *Sensors and Actuators B: Chemical* 134 2008: pp. 1034 – 1041. https://doi.org/10.1016/j.snb.2008.07.005
14. **Li, S., Zhao, B., Aguirre, A., Wang, Y., Li, R., Yang, S., Aravind, I., Cai, Z., Chen, R., Jensen, L.** Monitoring Reaction Intermediates in Plasma-Driven SO_2, NO, and NO_2 Remediation Chemistry Using In Situ SERS Spectroscopy *Analytical Chemistry* 2021: pp. 6421 – 6427. https://doi.org/10.1021/acs.analchem.0c05413
15. **Das, S., Girija, K., Debnath, A., Vatsa, R.** Enhanced NO_2 and SO_2 Sensor Response under Ambient Conditions by Polyol Synthesized Ni Doped SNO_2 Nanoparticles *Journal of Alloys and Compounds* 854 2021: pp. 157276. https://doi.org/10.1016/j.jallcom.2020.157276
16. **Hu, Y., Tan, O.K., Zhu, W., Cao, W.** Solid-state Gas Sensors *In Sensors for Chemical and Biological Applications*: CRC, Press New York. 2010: pp. 1 – 42.
17. **Wolfbeis, O.S., Reisfeld, R., Oehme, I.** Sol-gels and Chemical Sensors *Optical and Electronic Phenomena in Sol-Gel Glasses and Modern Application* 1996: pp. 51 – 98.
18. **Arcibar-Orozco, J.A., Rangel-Mendez, J.R., Bandosz, T.J.** Reactive Adsorption of SO_2 on Activated Carbons with Deposited Iron Nanoparticles *Journal of Hazardous Materials* 246 2013: pp. 300 – 309.

https://doi.org/10.1016/j.jhazmat.2012.12.001

19. **Kim, J., Kim, H.I., Yun, J.** Improvement of Gas Sensing Properties of Carbon Nanofibers Based on Polyacrylonitrile and Pitch by Steam Activation *Carbon Letters* 24 2017: pp. 36 – 40. https://doi.org/10.5714/CL.2017.24.036
20. **Ingle, N., Sayyad, P., Deshmukh, M., Bodkhe, G., Mahadik, M., Al-Gahouari, T., Shirsat, S., Shirsat, M.D.**. A Chemiresistive Gas Sensor For Sensitive Detection of SO_2 Employing Ni-MOF Modified–OH-SWNTs and–OH-MWNTs *Applied Physics A* 127 2021: pp. 1 – 10. https://doi.org/10.1007/s00339-021-04288-0
21. **Giordani, S.** Recent Developments in Carbon Nanomaterial Sensors *Chemical Society Reviews* 44 2021: pp. 4433 – 4453. https://doi.org/10.1039/C4CS00379A
22. **Salih, E., Ayesh, A.I.** Sensitive SO_2 Gas Sensor Utilizing Pt-Doped Graphene Nanoribbon: First Principles Investigation *Materials Chemistry and Physics* 2021: pp. 124695. https://doi.org/10.1016/j.matchemphys.2021.124695
23. **Hu, J., Zou, C., Su, Y., Li, M., Hu, N., Ni, H., Yang, Z., Zhang, Y.** Enhanced NO_2 Sensing Performance of Reduced Graphene Oxide by in Situ Anchoring Carbon Dots *Journal of Materials Chemistry C* 5 2017: pp. 6862 – 6871. https://doi.org/10.1039/C7TC01208J
24. **Peng, S., Cho, K.** Ab Initio Study of Doped Carbon Nanotube Sensors *Nano Letters* 3 2003: pp. 513 – 517. https://doi.org/10.1021/nl034064u
25. **Nagarajan, V., Chandiramouli, R.** A Novel Approach for Detection of NO_2 and SO_2 Gas Molecules Using Graphane Nanosheet and Nanotubes. A Density Functional Application *Diamond and Related Materials* 85 2018: pp. 53 – 62. https://doi.org/10.1016/j.diamond.2018.03.028
26. **Yoosefian, M., Zahedi, M., Mola, A., Naserian, S.** A DFT Comparative Study of Single and Double SO_2 Adsorption on Pt-Doped and Au-Doped Single-Walled Carbon Nanotube *Applied Surface Science* 349 2015: pp. 864 – 869. https://doi.org/10.1016/j.apsusc.2015.05.088
27. **Kim, S., Lee, J.Y.** Doping and Vacancy Effects of Graphyne on SO_2 Adsorption *Journal of Colloid and Interface Science* 493 2017: pp. 123 – 129. https://doi.org/10.1016/j.jcis.2017.01.019
28. **Grimme, S., Ehrlich, S., Goerigk, L.** Effect of the Damping Function in Dispersion Corrected Density Functional Theory *Journal of Simulational Chemistry* 32 2011: pp. 1456 – 1465. https://doi.org/10.1002/jcc.21759
29. **Ma, R., Ren, X., Xia, B.Y., Zhou, Y., Sun, C., Liu, Q., Liu, J., Wang, J.** Novel Synthesis of N-Doped Graphene as an Efficient Electrocatalyst Towards Oxygen Reduction *Nano Research* 9 2016: pp. 808 – 819. https://doi.org/10.1007/s12274-015-0960-2
30. **Joucken, F., Tison, Y., Le Fèvre, P., Tejeda, A., Taleb-Ibrahimi, A., Conrad, E., Repain, V., Chacon, C., Bellec, A., Girard, Y.** Charge Transfer and Electronic Doping in Nitrogen-Doped Graphene *Scientific Reports* 5 2015: pp. 14564. https://doi.org/10.1038/srep14564
31. **Zhao, C., Zhou, X., Xie, S., Wei, H., Chen, J., Chen, X., Chen, C.** DFT study of electronic structure and properties of N, Si and Pd-doped carbon nanotubes *Ceramics International* 44 (17) 2018: pp. 21027 – 21033. https://doi.org/10.1016/j.ceramint.2018.08.138
32. **Gecim, G., Ozekmekci, M., Fellah, M.F.** Ga and Ge-doped Graphene Structures: A DFT Study of Sensor Applications for Methanol *Computational and Theoretical Chemistry* 1180 2020: pp. 112828. https://doi.org/10.1016/j.comptc.2020.112828
33. **Aslan, M.** Structural, Electronic and Magnetic Properties of Bimetallic Pdco Nanoparticles with/without Metal Oxide Support and Their Interactions with Nitric Oxide (NO): A First Principle (Ab Initio) Material Modeling Study *Journal of Nanoparticle Research* 21 (11) 2020: pp. 1 – 19. https://doi.org/10.1007/s11051-019-4636-9
34. **Tarique, M.** Probing the Binding Fashion in Coordination Compounds of D-Block Metals with Versatile Dithiocarbamate N and S Containing Ligand *Advanced Journal of Science and Engineering* 1 2020: pp. 12 – 15.
35. **Mirzaei, M., Karimi, E., Yousefi, M.** BN Nanoflake for Hazardous SO_2 Gas Capturing *DFT Study* 12 2022: pp. 359 – 365. https://doi.org/10.33263/BRIAC121.359365
36. **Moezi, E., Mirzaei, M.** Graphene scaffold for tioguanine delivery: DFT approach Lab-in-Silico 2 (1) 2021: pp. 25 – 29. https://doi.org/10.22034/labinsilico21021025
37. **Harismah, K., Ozkendir, O.M., Mirzaei, M.** DFT Studies of Single Lithium Adsorption on Coronene *Zeitschrift für Naturforschung A* 73 (8) 2018: pp. 685 – 691. https://doi.org/10.1515/zna-2017-0458
38. **Tarique, M.** Probing the Binding Fashion In Coordination Compounds of D-Block Metals with Versatile Dithiocarbamate N and S Containing Ligand *Advanced Journal of Science and Engineering* 1 2020: pp. 12 – 15. http://doi.org/10.22034/AJSE2013074
39. **Aslan, M.** Bimetallic AuM (M=Ni and Ag) Clusters/nanoparticles and their Extended (111) Surfaces for NO_2 Adsorption: A Computational Material Study *Materials Today Communications* 26 2021: pp. 101821. https://doi.org/10.1016/j.mtcomm.2020.101821
40. **Aslan, M., Johnston, R.L.** Anionic Cobalt-platinum-ethynyl (Copt–C2H) Metal-Organic Subnanoparticles: A DFT Modeling Study *The European Physical Journal B* 91 2018: pp. 1 – 9. https://doi.org/10.1140/epjb/e2018-90004-2